Available online at www.sciencedirect.com
ScienceDirect
Icarus 194 (2008) 278–289
ICARUS
www.elsevier.com/locate/icarus

Moonlets and clumps in Saturn's F ring

Larry W. Esposito [a,*], Bonnie K. Meinke [a], Joshua E. Colwell [b], Philip D. Nicholson [c], Matthew M. Hedman [c]

[a] *Laboratory for Atmospheric and Space Physics, University of Colorado, 392 UCB, Boulder, CO 80309, USA*
[b] *Department of Physics, University of Central Florida, Orlando, FL 32816, USA*
[c] *Astronomy Department, Cornell University, Ithaca, NY 14853, USA*

Received 13 September 2007; revised 24 September 2007

Available online 22 October 2007

Abstract

Cassini UVIS star occultations by the F ring detect 13 events ranging from 27 m to 9 km in width. We interpret these structures as likely temporary aggregations of multiple smaller objects, which result from the balance between fragmentation and accretion processes. One of these features was simultaneously observed by VIMS. There is evidence that this feature is elongated in azimuth. Some features show sharp edges. At least one F ring object is opaque and may be a "moonlet." This possible moonlet provides evidence for larger objects embedded in Saturn's F ring, which were predicted as the sources of the F ring material by Cuzzi and Burns [Cuzzi, J.N., Burns, J.A., 1988. Icarus 74, 284–324], and as an outcome of tidally modified accretion by Barbara and Esposito [Barbara, J.M., Esposito, L.W., 2002. Icarus 160, 161–171]. We see too few events to confirm the bi-modal distribution which Barbara and Esposito [Barbara, J.M., Esposito, L.W., 2002. Icarus 160, 161–171] predict. These F ring structures and other youthful features detected by Cassini may result from ongoing destruction of small parent bodies in the rings and subsequent aggregation of the fragments. If so, the temporary aggregates are 10 times more abundant than the solid objects. If recycling by re-accretion is significant, the rings could be quite ancient, and likely to persist far into the future.

Keywords: Accretion; Occultations; Saturn, rings; Ultraviolet observations

1. Introduction

The F ring is well known to be unusual, with multiple strands, kinks, clumps and even "braids" where the strands appear to cross (Smith et al., 1982; Murray et al., 1997). Multiple lines of evidence show a range of particle sizes, from dust to some objects 1 km across. Showalter et al. (1992) described the F ring as a core of centimeter-sized particles within a wider envelope of much smaller micron-sized dust. Cuzzi and Burns (1988) explained the abrupt depletions in magnetospheric particles seen by Pioneer 11 experiments as due to small moonlets (0.1–10 km in radius) in a belt 2000 km wide surrounding the F ring. During the 1995/1996 edge-on orientation of the ring, numerous small bodies were reported within the F ring (Bosh and Rivkin, 1996; Nicholson et al., 1996). However, a number of characteristics (their size, brightness and in some cases disappearance) are inconsistent with solid bodies (Poulet et al., 2000). Showalter (1998, 2004) reanalyzed 1980 and 1981 Voyager images of Saturn's F ring with special attention to very transient bright features he called "burst" events. Showalter interpreted these phenomena as dust clouds created by meteoroid bombardment of the ring. Barbara and Esposito (2002), using an updated version of Cuzzi and Burns (1988) model that includes both accretion and fragmentation, have criticized this explanation. They interpret the bright burst events as due to disruptive collisions between unconsolidated parent bodies in the F ring. In their model, the competition between accretion and fragmentation results in a bi-modal distribution with abundant dust as well as a significant number of larger bodies. Canup and Esposito (1995) showed that at the F ring's distance from Saturn, tides hamper accretion, so that the two colliding bodies become gravitationally bound only if they differ significantly in mass.

* Corresponding author. Fax: +1 303 492 1132.
E-mail address: larry.esposito@lasp.colorado.edu (L.W. Esposito).

0019-1035/$ – see front matter
doi:10.1016/j.icarus.2007.10.001

The F ring is therefore an interesting locale to test ring history. Although accretion can occur inward of the F ring (see Karjalainen, 2007), it is particularly evident in the optically thin F ring itself. Solid bodies and any other aggregations are evident not only by their brightness in reflected sunlight, as observed by Showalter (1998, 2004), but their opacity to starlight in a ring occultation (Esposito et al., 1998). The brightenings studied by Showalter may be caused by dust liberated from larger objects, and thus indirect evidence for physical clumps or moonlets. This paper describes evidence for dense concentrations of material, the discovery of at least one opaque feature, and thus of potentially solid objects in Saturn's F ring. These objects have implications for the dynamics and history of the F ring.

2. UVIS F ring occultations

The Cassini Ultraviolet Imaging Spectrograph (UVIS) has a separate high-speed photometer (HSP) channel for observing star occultations (Esposito et al., 1998, 2004, 2005). The effective wavelength for this channel is about 1500 Å. As of 15 June 2007, UVIS has observed 60 star occultations, which provide 44 radial cuts measuring the opacity profile of the F ring. Together, these provide measurements of the F ring's transparency to starlight at a variety of longitudes, times and angles (Colwell et al., 2006, 2007). These observations show the F ring opacity varies with time and allows us to identify many individual structures. Some of these structures are expected from previous Voyager observations (Lane et al., 1982; Smith et al., 1982; Murray et al., 1997; Showalter, 2004). Although we find broad features consistent with multiple "strands" of the F ring, we also see smaller structures that are not repeatable, each appearing in only one radial occultation profile. In lieu of repeated or long-term observations, which are not possible with occultation data, the opacity of the feature may be used as a proxy for its longevity. The apparently opaque features are more likely to be solid, "permanent" objects, which we will refer to loosely as "moonlets," while the less opaque ones we refer to as "clumps," because they are likely to be more ephemeral. The relationship between any of these features and those observed in multiple Cassini images, such as S/2004 S6, is presently unclear. We identify the single, opaque event we have detected with a possible moonlet.

3. Search method

To efficiently search for narrow, transient features in the F ring and distinguish these from simple noise variations, we first considered an object that could be independently verified as a clump. Such an event occurred during Cassini rev 13 with the occultation of α Sco, which was observed by both the VIMS (Hedman et al., 2007) and UVIS instruments. Although primarily an imaging spectrometer, VIMS can also operate in "stellar occultation mode," when it stares at a single 0.25 by 0.5 mrad pixel and takes 1–5 micron spectra at intervals as short as 20 ms (Brown et al., 2004). Both UVIS and VIMS detected an especially notable increase in the ring opacity about 500 m wide, which we have nicknamed "Pywacket." The simultaneous detection in the UV and near IR (2.92 μm effective wavelength) assures this is not merely a statistical fluctuation, but a real feature in the F ring. A plot of the VIMS and UVIS occultation data in Fig. 1 shows this feature at a radial distance of 140,552 km from Saturn in the plane of the F ring defined by Bosh et al. (2002), about 10 km exterior to the F ring core.

The star α Sco is actually a double star, with α ScoA visible only to VIMS and α ScoB visible only to UVIS. Because the two stars crossed the same radial distance at a separation of about 600 m in longitude (including the orbital motion of the particles) Pywacket must be significantly elongated, like many features seen previously in Voyager (Showalter, 2004) and Cassini (Murray, 2006) images. A spherical object could only match these observations if the midpoint of the binary stars fortuitously passed very close to the sphere's center. If the object were ellipsoidal, this implies an axial ratio greater than 2. Pywacket is 25 samples wide in the UVIS occultation, and 2 samples in VIMS. The possible shoulder inward of Pywacket in Fig. 1 may also indicate unconsolidated material associated with this clump.

We have used this confirmed detection to refine our search algorithm for similar features in the UVIS data. The method to flag significant features is entirely automated, as follows. The data are first binned into sums of 5 consecutive integration periods, with typically 2 ms integrations. We take a running mean from the 81 bins of stellar signal surrounding and including each data bin, in order to determine a smoothed baseline for the F ring opacity. Assuming the signal is described by a Poisson distribution, where μ corresponds to the baseline value and C is the binned stellar signal at a particular bin, the probability of measuring a value of exactly C is given by

$$P(\mu, C) = \frac{e^{-\mu}\mu^C}{C!}. \tag{1}$$

To find the probability that the stellar signal would be less than or equal to C at that bin, we sum the distribution over all signal values less than C:

$$P(\mu, \leqslant C) = \sum_{j=0}^{C} \frac{e^{-\mu}\mu^j}{j!}. \tag{2}$$

We perform this for each bin, i, in the data set to find $P_i = P(\mu_i \cdot C_i)$. We then multiply P_i by the number of tested bins in the data set, N. This gives $m = NP_i$ (Colwell et al., 1990). Events with $m < 1$ are statistically significant, and are flagged for the "persistence" test, as follows. Each flagged event is examined to determine its width and peak opacity. To be included on our list, the maximum binned normal optical depth in the feature must be at least as large as Pywacket ($\tau_{\max} = 0.4$ when binned over 5 integration periods). We apply this test to all 44 occultation profiles of the F ring. This yields 13 events, distributed in radial width from 27 m to 9 km (see Table 1). For stationary spheres, this radial width would underestimate the true diameter on the average by about 20%, since the average chord length is $\pi/4$ times the diameter. Since the clumps are likely moving at Keplerian velocity (comparable to the projected star speed) this radial width (the difference in radius

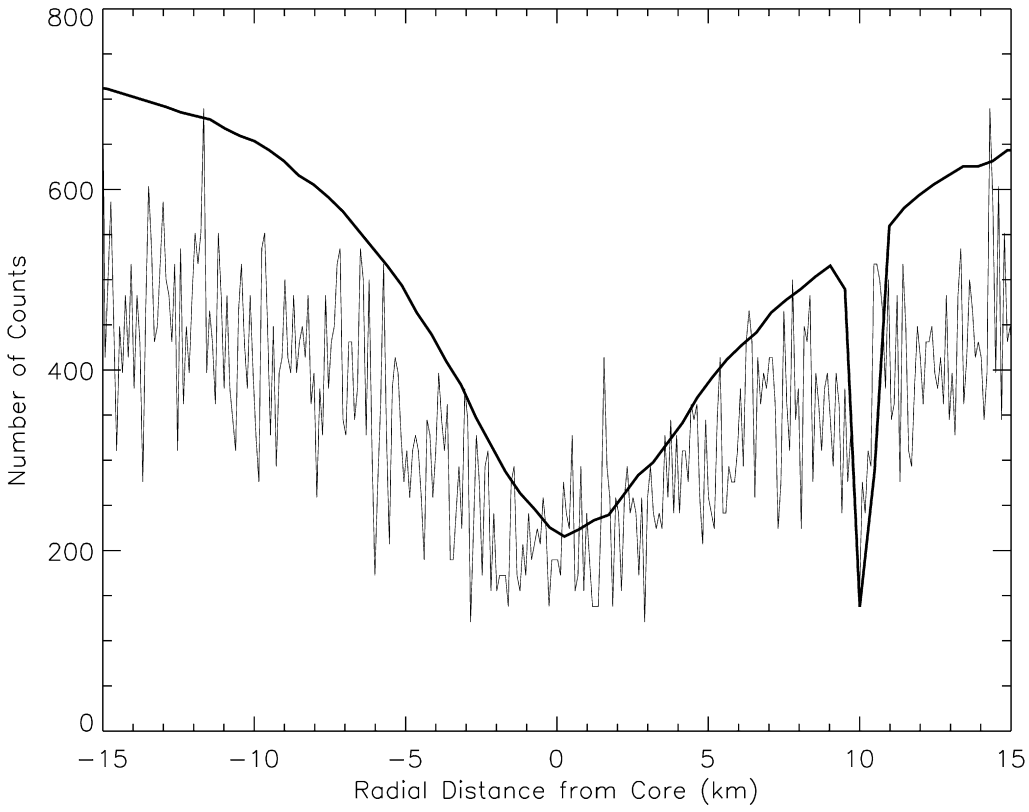

Fig. 1. VIMS (solid, smooth black curve) and UVIS (thin, gray curve) alpha Sco Egress occultation data overplotted. The UVIS data curve (scaled to match VIMS unocculted flux far from the event, off the figure) appears noisier, but at the center of the event has higher spatial resolution. Pywacket, the event 10 km outside the F ring core, is detected by both instruments.

Table 1

Event #	Occultation (rev)	Ephemeris time	Peak normal optical depth	Equivalent depth (km)	Radial distance (km)	B (deg) [declination wrt rings]	Projected star diameter (m)	Longitude	dR (km)	Radial width (m)
1 (Mittens)	alp Leo (9)	171479259	> 0.8	> 0.4	139,917	9.537	3	350.5	4.29	600
2	126 tau (8)	169784293	1.6	0.04	140,067	21.063	2	227.2	0.57	30
3	126 tau (8)	169784293	1.2	0.05	140,067	21.063	2	227.2	0.66	60
4 (Pywacket)	alp Sco (13) Egress	177819530	0.4	0.04	140,552	32.160	36	10.0	10.63	500
5 (Butterball)	alp Vir (34) Egress	218390789	0.7	0.64	140,161	−17.249	2	89.4	−1.40	1100
6 (Fluffy)	alp Vir (34) Egress	218390789	0.8	0.91	140,162	−17.249	2	89.4	0	1400
7	gam Ara (37) Ingress	222702085	1.2	0.04	140,282	−60.998	3	248.4	3.40	40
8	gam Ara (37) Ingress	222702085	2.2	1.55	140,280	−60.998	3	248.4	2.66	1020
9	gam Ara (37) Ingress	222702086	> 4.9	> 24.91	140,274	−60.998	3	248.4	0	9000
10	chi Cen (39)	225706472	0.4	0.02	139,911	55.084	2	258.5	−13.0	180
11	the Ara (41)	227605973	0.6	0.02	140,406	−53.858	2	59.8	3.0	180
12	bet Per (42)	229319343	0.5	0.03	140,236	47.370	2	46.6	178.4	60
13	zet Oph (26)	207062459	0.8	0.21	139,894	−16.215	2	0.06	0	260

Notes. Ephemeris time values are seconds from the J2000 epoch. Equivalent depth: The radial integral of optical depth across the feature. Longitudes and reference radii were computed using the eccentric, inclined F ring model of Bosh et al. (2002). Longitudes are calculated prograde from the ring ascending node of J2000. dR is the radial position relative to the observed F ring core reference radius ($R0$): α Leo $R0 = 139{,}913$ km; 126 Tau (8) $R0 = 140{,}066$ km; α Sco $R0 = 140{,}542$ km; α Vir $R0 = 140{,}162$ km; γ Ara $R0 = 140{,}274$ km; χ Cen $= 139{,}924$ km; θ Ara $= 140{,}403$ km; β Per $R0 = 140{,}414$ km; ζ Oph $= 139{,}894$ km.

between the first and last event points) provides a lower limit to the true dimensions.

The radial width is the full width of all consecutive bins that meet the m test significance criterion, $m < 1$. Peak optical depth is the maximum from the binned data. An identical test of similar duration (100 km in length, which represents 500–1000 bins, depending on the occultations) from observations of the same stars when not occulted by known rings gives no flagged events. Searches where the data are tested in different size bins give similar results. We conclude that these 13 events almost certainly represent real structures in the F ring. Because of the optical depth requirement, $\tau > 0.4$, the ring particles in such aggregations must collide multiple times each orbit (Shu and Stewart, 1985). The collision rate is proportional

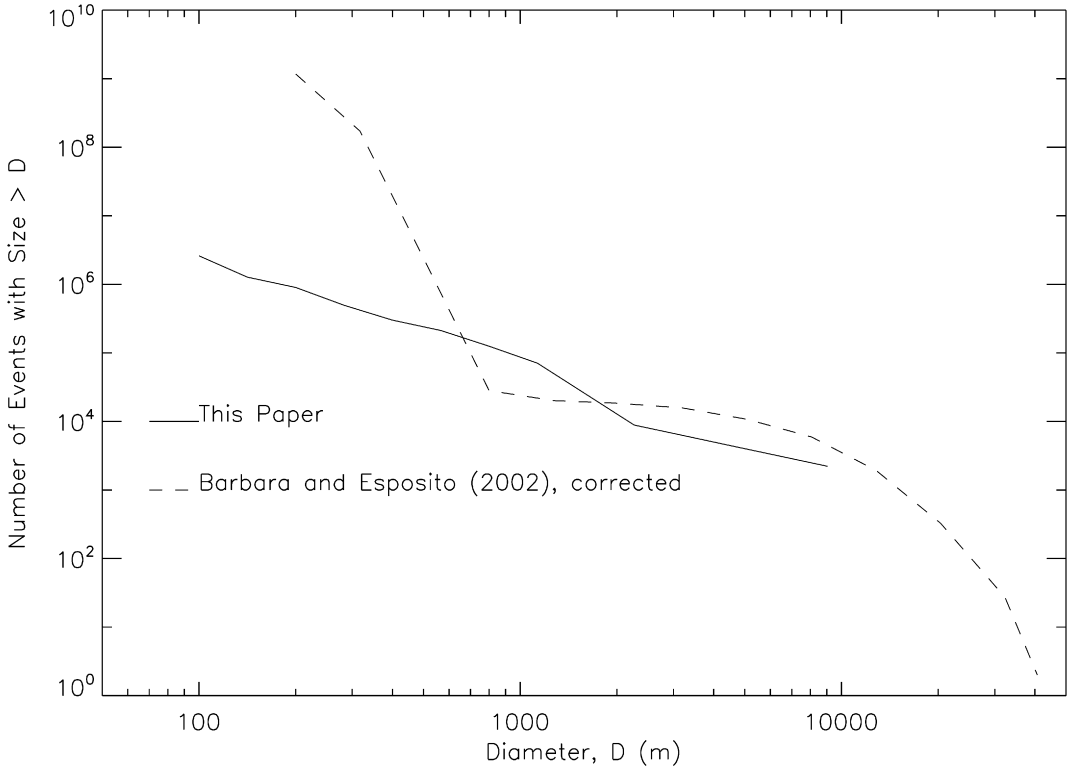

Fig. 2. Cumulative size distribution of events scaled to entire F ring found in this study, compared to simulations by Barbara and Esposito (2002). The model results are corrected to give an optical depth 0.1 in the F ring. The events found in this study show no evidence of a bi-modal distribution.

to the observed optical depth, τ, and the number of collisions for a particle to escape the clump is proportional to τ^2. The clump lifetime is estimated by the ratio, and thus scales as the clump optical depth, τ. Since an aggregation disappears when its members diffuse apart through collisions, this means that these more opaque structures will persist for multiple orbits. The size distribution of our 13 events is plotted in logarithmic size bins in Fig. 2. The size is the measured radial width (Table 1). The results have been scaled to the whole F ring, and are compared to previous results by Barbara and Esposito (2002), which were corrected to give a total optical depth of $\tau = 0.1$ for the F ring.

4. Opaque event

One of our events from the alpha Leonis occultation, nicknamed "Mittens," is an opaque feature 600 m (21 integration periods) wide at a distance of 139,917 km in the F ring plane. See Figs. 3 and 4. This is our best candidate for a "moonlet," that is, a solid, more permanent structure in the F ring. Such moonlets may provide the unseen mass that is the source of the visible ring material, as proposed by Cuzzi and Burns (1988). The coordinates of this event do not match any other moonlets like S/2004 S6 or other structures seen by Cassini cameras (Murray, 2006). The other 12 features are not so clearly opaque. Feature 6, "Fluffy," has roughly symmetric flanks and may be the F ring core, resembling features seen in other occultations at the inferred center of the F ring. Features 5 and 9 (Figs. 5 and 6) both have minimum counting rates within one standard deviation of the calculated background level, so they possibly contain opaque regions. Features 7, 8 and 9 are shown in Fig. 6. These features are not so distinctive as Mittens, and thus are much more likely temporary aggregations that may resemble the self-gravity wakes seen in other rings (Colwell et al., 2007), and may be like those that cause the brightness increases seen by Voyager (Showalter, 1998). We envision these as elongated temporary features, although how elongated and temporary is not known. Feature 9 may just be the F ring core. From our measurement of one 600 m moonlet, Mittens, in one of 44 independent cuts, we estimate 3×10^4 such moonlets in the F ring, providing a total optical depth of 3×10^{-4} in such objects, over a width of 50 km for the F ring. We have

$$N = \frac{n_{\rm obs}}{n_{\rm occ}} \frac{2\pi R}{W_{\rm obs}}, \tag{3}$$

$$\tau = \frac{n_{\rm obs}}{n_{\rm occ}} \frac{W_{\rm obs}}{\Delta R}, \tag{4}$$

where $n_{\rm obs}$ is the number of observed events ($n_{\rm obs} = 1$), $n_{\rm occ}$ is the number of occultation cuts ($n_{\rm occ} = 44$), $W_{\rm obs}$ is the observed event width and R and ΔR are the Saturnocentric distance and width of the F ring.

If such objects are uniformly distributed, the Poisson distribution [Eq. (1)] also applies to the probability of detecting a feature in our occultations. If events like Mittens are Poisson distributed, P is now the probability that it blocks an occultation. We are trying to determine number of expected events, μ, which is estimated from our single event.

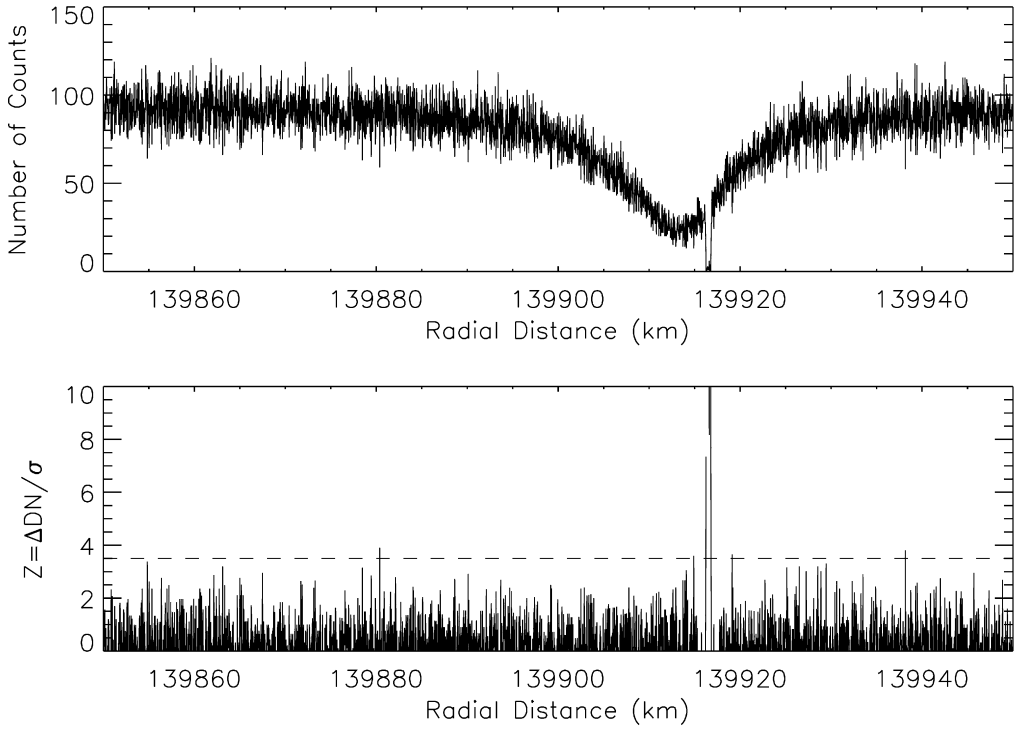

Fig. 3. Top: Raw data from the alpha Leonis F ring occultation. Bottom: Results of automated search with $Z_{\min} = 3.5$. Mittens is a more than 10-sigma event.

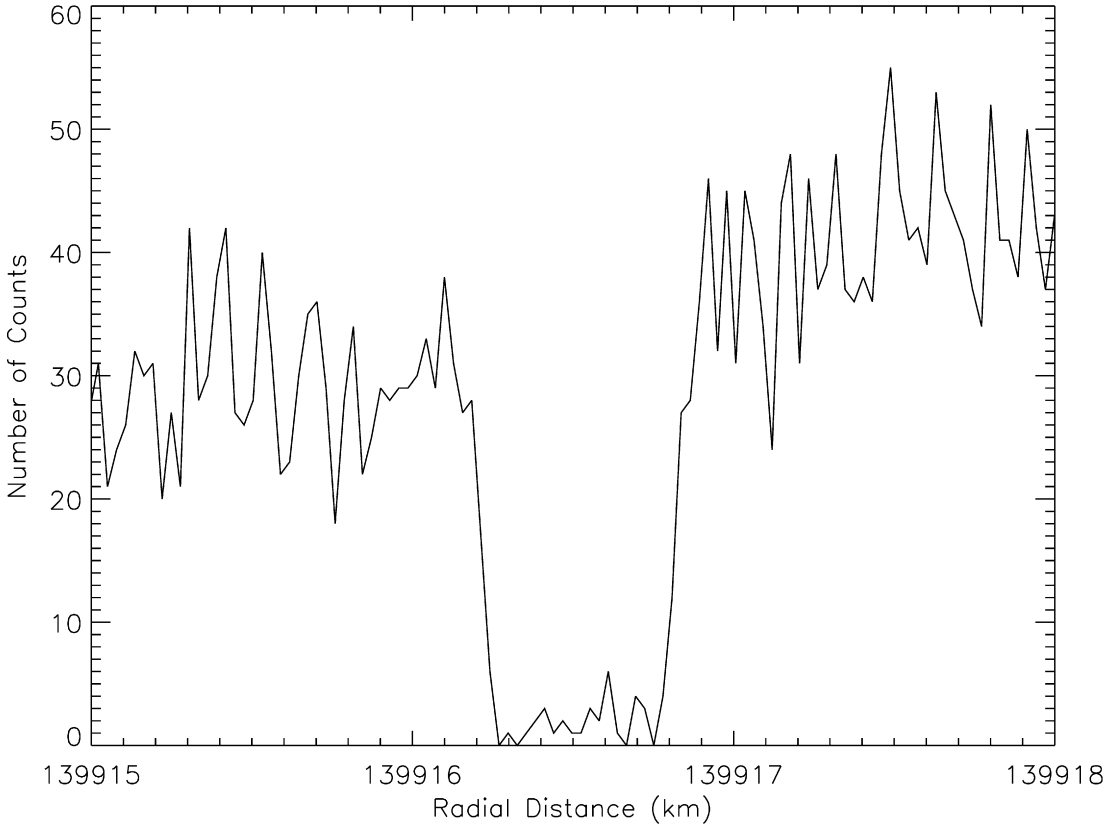

Fig. 4. Raw (unbinned) data of the alpha Leonis event Mittens (feature 1). The profile is consistent with an opaque moonlet.

For one observed event, $C = 1$. Equation (4) gives less than 5% probability of detecting one event if the expected number is either greater by 4.5, or conversely less by 20 times than the derived estimate. This gives 90% confidence that the number of objects like Mittens lies between 1.5×10^3 and 1.4×10^5.

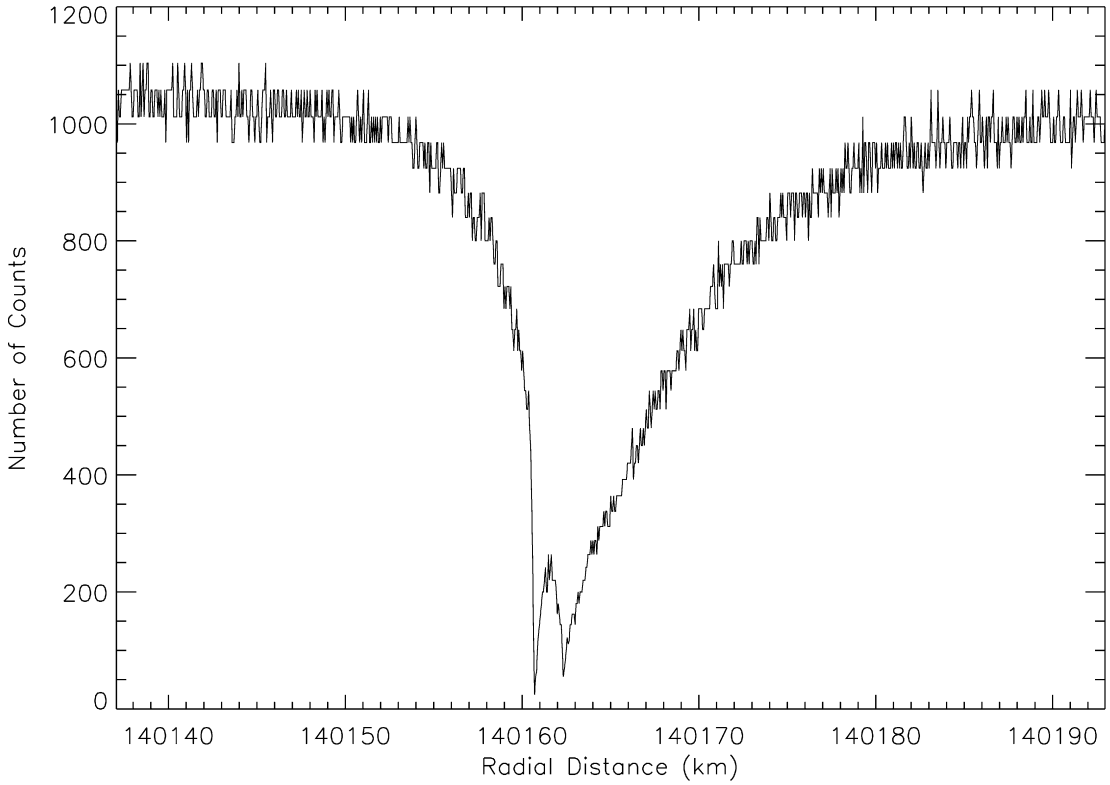

Fig. 5. Close-up view of the features 5 ("Butterball") and 6 ("Fluffy") from alpha Vir (rev 34).

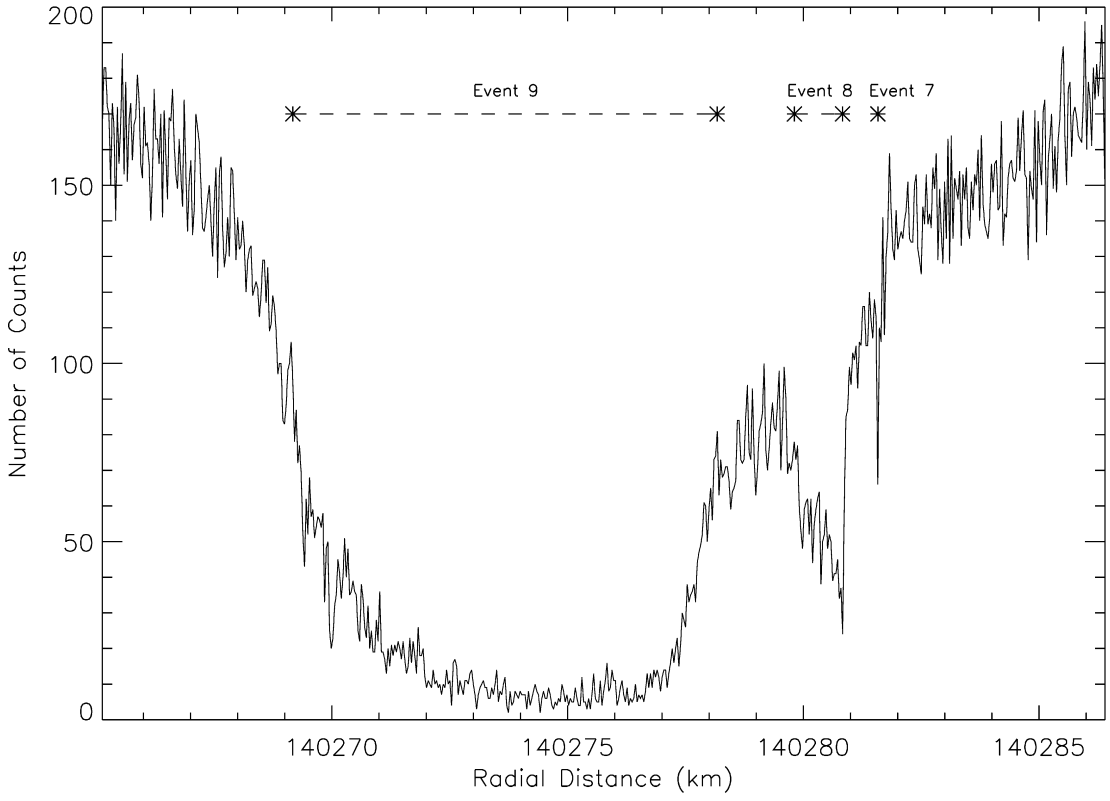

Fig. 6. Features 7, 8, 9 from gamma Ara. Note the sharp edges of features 7 and 8, resembling Mittens in Fig. 4. Feature 9 may just be a manifestation of the F ring core at this particular time and longitude.

5. Clumps

Examination of the events in Table 1 (see Figs. 4–12) shows a broad diversity. Features are seen inside, outside, and at the F ring core location. Widths range from 27 m to 1.4 km (excluding event 9, which may be only a broad manifestation of the F ring core). Pywacket may be elongated azimuthally. Peak optical depths and equivalent widths (the integral of the optical depth across the feature) vary by more than an order of magnitude. If these events represent transient features, they occur in a variety of times, shapes and locations. Disruption of such structures could explain the bright burst events seen by Voyager (Showalter, 2004; Barbara and Esposito, 2002).

The 13 features we have observed appear to fall into four different morphological groups. Two features (6, 13) appear to be a highly peaked central F ring core, while another is an exceptionally wide and optically thick core. Most features (9 of 13 features) are observed as sharp increases in optical depth in comparison to the surrounding occultation profile. Feature 8 has one sharp edge, while the other shoulder is a gradual signal decrease. Perhaps one side of this clump is more loosely aggregated. We also see differing edges for features 4 (Pywacket) and feature 5, which have sharp inner edges, and feature 8, which has a sharp outer edge. We also observe a single opaque feature with sharp edges in the occultation profile, Mittens, our best moonlet candidate.

The three core-overlapping events that our statistical and persistence tests flagged may be due to the "braided" nature of the F ring (Murray et al., 1997). As different strands overlap it is possible that the central core of the F ring grows wider and denser (event 9) or that the core reduces to a narrow, sharp strand (events 6 and 13) as other strands move away from the core.

The other 10 features in our data set do not appear to be related to known structures in the F ring. Rather, these events occur outside the core of the ring and are small in comparison to the width of the entire F ring core. Most of these events also have sharp edges in the occultation profile, which makes them appear to be self-contained structures and not just small density enhancements in the overall ring structure.

From the Cassini perspective, we may wish to reconsider the Voyager stellar and radio occultations of the F ring (Lane et al., 1982; Tyler et al., 1981). Both showed a narrow opaque "core" that has not been seen in the Cassini results. It is possible that these events might now better be interpreted as possible clumps! For the radio science results, this would imply particles in the clump larger than centimeter size.

6. Comparison to observations, models

The estimated number of such objects like Mittens is about the same as for the propeller-creating objects inferred by Tiscareno et al. (2006). However, Mittens is 10 times larger. Thus, objects like it would be three orders of magnitude more abundant than the extrapolated size distribution from the region of Saturn's A ring imaged by Tiscareno et al. This could be an indication of more effective accretion further from Saturn in the F ring.

Barbara and Esposito (2002) considered the equilibrium between the processes of fragmentation and accretion in Saturn's F ring to explain the occasional brightenings seen by Voyager (Showalter, 1998). Our current results are too few to provide a confirmation of their predictions of a bi-modal size distribution. However, the data in Fig. 2 do not show a steep power law distribution with index $q = 5$, which Tiscareno et al. extrapolate in the A ring, at least at the sizes detected by UVIS star occultations. Tiscareno's objects are 10,000 km closer to Saturn, in the outer A ring, and may be the result of a recently disrupted moon (Sremcevic et al., 2007). If the F ring objects form by accretion (Barbara and Esposito, 2002), we would not expect such a steep distribution. A flatter distribution is more consistent with our observations. The flat shape of the observed distribution gives a good indication that any initially steep power law distribution produced by the disruption of a parent object to form the F ring (Cuzzi and Burns, 1988) has been modified by accretion.

We do not yet detect any large bodies outside the present F ring, as predicted by Cuzzi and Burns. This is not a contradiction of their model: their predicted number (which depends on their undetermined moonlet size) could easily fall below our detection sensitivity.

7. Models of ring recycling and evolution

Calculations by Canup and Esposito (1995, 1997), Throop and Esposito (1998) and Barbara and Esposito (2002) show that the balance between fragmentation and accretion leads to a bi-modal size distribution in the Roche zone, where a small number of larger bodies coexist with the ring particles and dust. Thus, after disruption, some significant mass fraction of a shattered moonlet would be recaptured by other moonlets and is available for producing future rings. If the recycling is large enough, this can indefinitely extend the ring lifetime (Esposito and Colwell, 2003, 2004, 2005; Esposito, 2006). Larger bodies in the Roche zone can gradually grow if they can attain a roughly spherical shape (Ohtsuki, 2002). Those that do stick will continue to grow, perhaps until they are large enough to form a propeller structure (Spahn and Sremcevic, 2000; Sremcevic et al., 2002). The growth process, including many starts and stops, disruptions and rare events, may be very slow: we call this "creeping" growth.

8. Discussion

Structures observed in Saturn's rings indicate active processes and provide constraints on the ring history and ring origins (Esposito, 1986; Spahn and Wiebicke, 1989; Cuzzi and Estrada, 1998; Esposito, 2006). Cassini has provided a closer view of the rings, bringing into our view new structure in the rings. This includes straw-like aggregations (Porco et al., 2005), compositional variations (Esposito et al., 2005; Brown et al., 2006), propeller-shaped structures (Tiscareno et al., 2006; Sremcevic et al., 2007), self-gravity wakes (Colwell et al., 2006, 2007; Hedman et al., 2007; Sremcevic et al., 2006), the

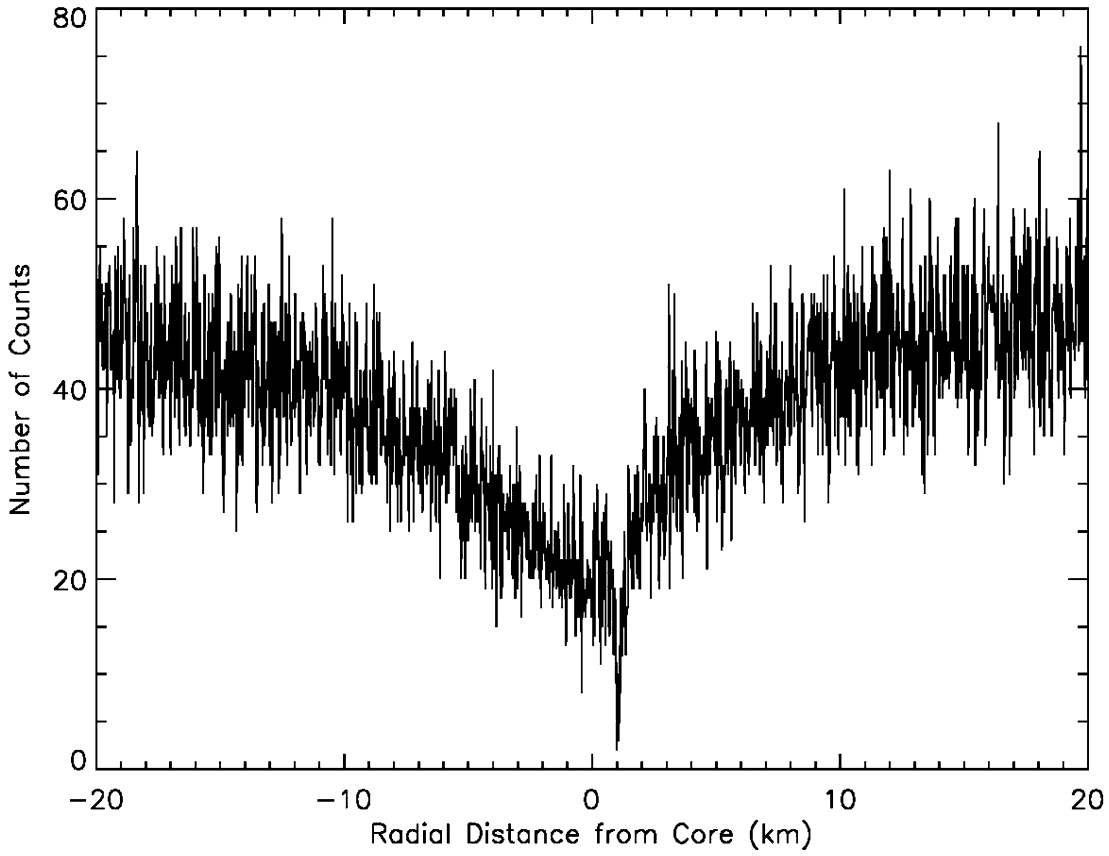

Fig. 7. Occultation by 126 Tau (rev 8), showing features 2 and 3.

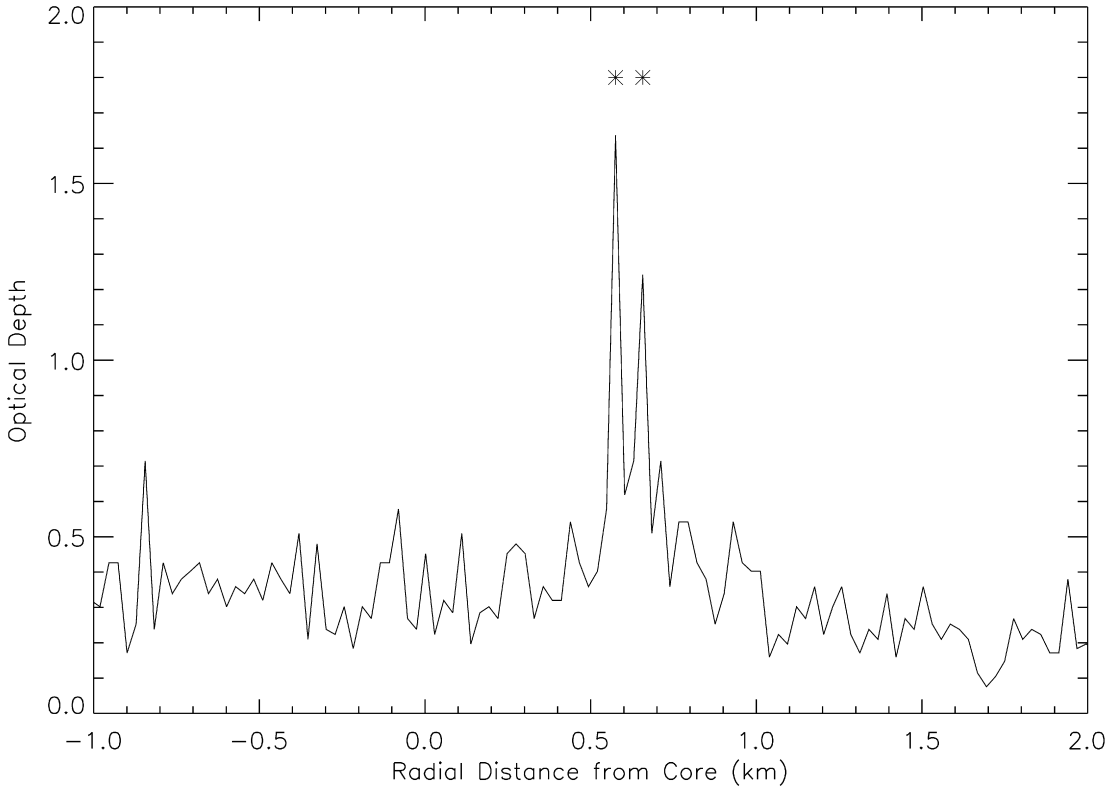

Fig. 8. Optical depth derived from data for 126 Tau (8), see Fig. 7.

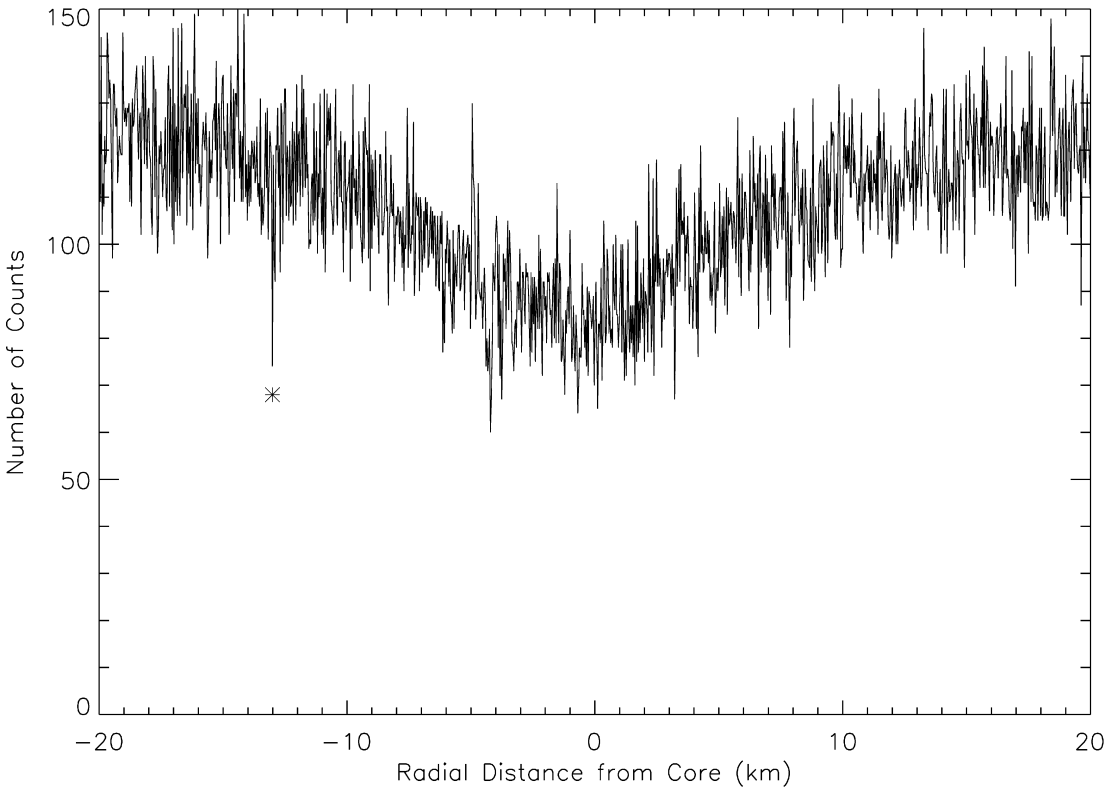

Fig. 9. Occultation data from chi Cen (rev 39). Feature 10 is marked by the asterisk.

low mass density of the Cassini Division inferred from density waves (e.g., Tiscareno et al., 2007) and discovery of new moons with average mass density less than solid ice (Porco et al., 2005, 2007; Porco, 2006). Ring edges and the D and F rings are significantly different from the Voyager observations just 25 years prior (Burns and Tiscareno, 2005). Movies of the F ring show embedded moonlets and temporary brightenings (Murray, 2006) extending the Voyager observations studied by Showalter (1998) and Barbara and Esposito (2002). These provide clear evidence for disruption of small bodies in the ring leading to new rings, as proposed by Esposito (1986), Esposito and Colwell (1989) and Colwell and Esposito (1992). Because the moonlet lifetime is so short (Colwell et al., 2000), either the rings must be very young (Dones, 1991; Esposito, 1986, 1991), or some process must continually produce these small bodies.

Current models do not consider the rare, random events that could lead to the establishment of a small moonlet that would be stable against tidal disruption. In fact, Barbara and Esposito (2002) did not distinguish at all between temporary and more permanent aggregations. These simulations should be improved by better nomenclature that clarifies the multiple states and by adding appropriate physics. A different numerical approach may be needed to handle the long timescales.

Recycling of ring material could also explain the limited micrometeoroid darkening of Saturn's rings (Cuzzi and Estrada, 1998). Why are the rings not darker now, if they are truly ancient? One possibility is that the total mass of the rings, mostly in Saturn's B ring, has been underestimated. Because the total opacity of the B ring is still unmeasured and may be more than two times greater than estimated (Colwell et al., 2007), meteoritic pollution would have a smaller effect. An important consideration is that meteoritic pollution affects mostly the exterior of objects. If the rings (particularly the B ring) are much more massive than we now estimate, the interior of the largest ring objects (which may encompass most of the ring mass) can remain more pristine until disrupted. The calculated short viscous diffusion timescales (e.g., Esposito, 1986) are also suspect because the clumping and instabilities change the viscosity (Colwell et al., 2007). Esposito (1986) noted that most of the age problems involve Saturn's A ring. Perhaps the A and F rings are more recent?

Another uncertainty is the exact magnitude of the bombarding flux, which is still poorly known. Attempts to observe the flash produced by 10 cm meteoroids onto the rings with the UVIS HSP yielded no detections, but this is due to the low flux of light in the HSP bandpass for such impacts (Chambers et al., 2007). Measurements by Cassini's Cosmic Dust Analyzer are dominated by dust in the Saturn system, primarily the E ring, and its cruise measurements did not allow for a determination of the micrometeoroid flux at Saturn (Srama et al., 2006; Altobelli, 2006). The New Horizons dust experiment should provide a useful measure of the heliocentric variation in micrometeoroid flux on its way to Pluto (Horanyi, personal communication, 2006).

9. Conclusion

Stellar occultations show features in Saturn's F ring consistent with predictions of larger bodies that may have formed by accretion. Most of the observed features are not opaque, and

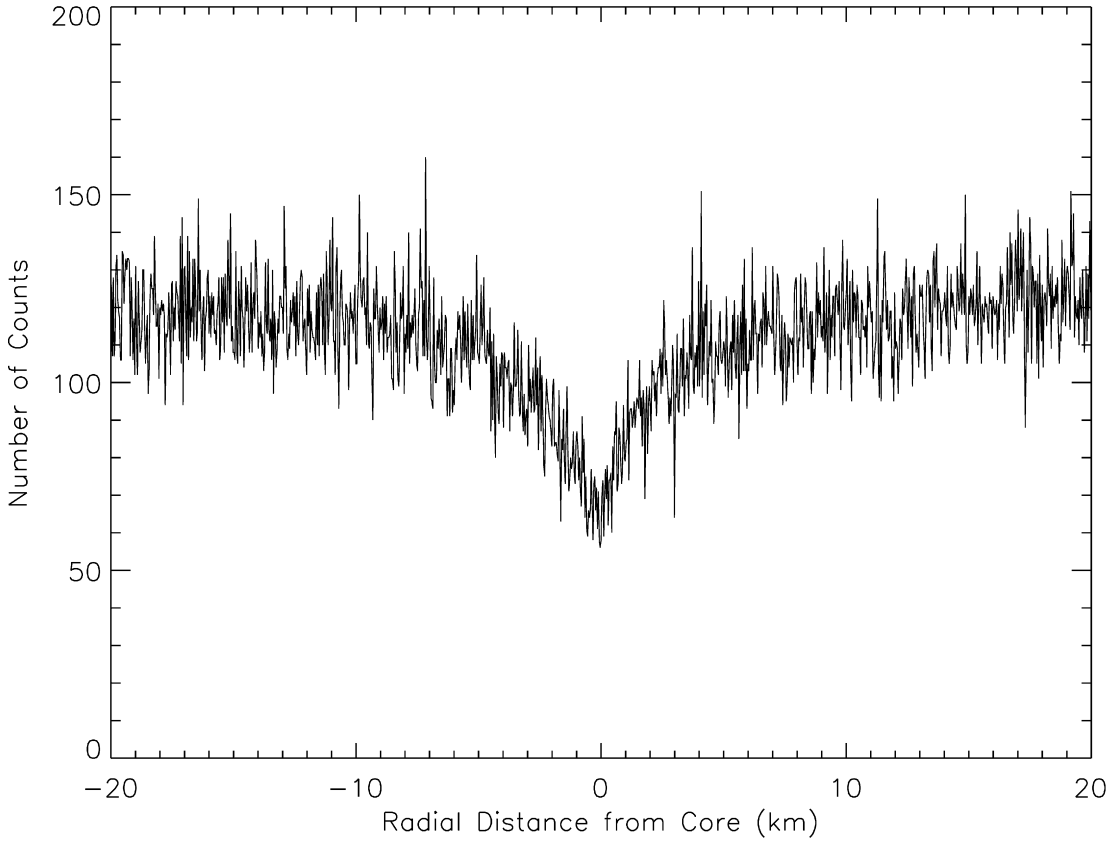

Fig. 10. Occultation data for theta Arae (rev 41). Feature 11 is 3 km outside the core.

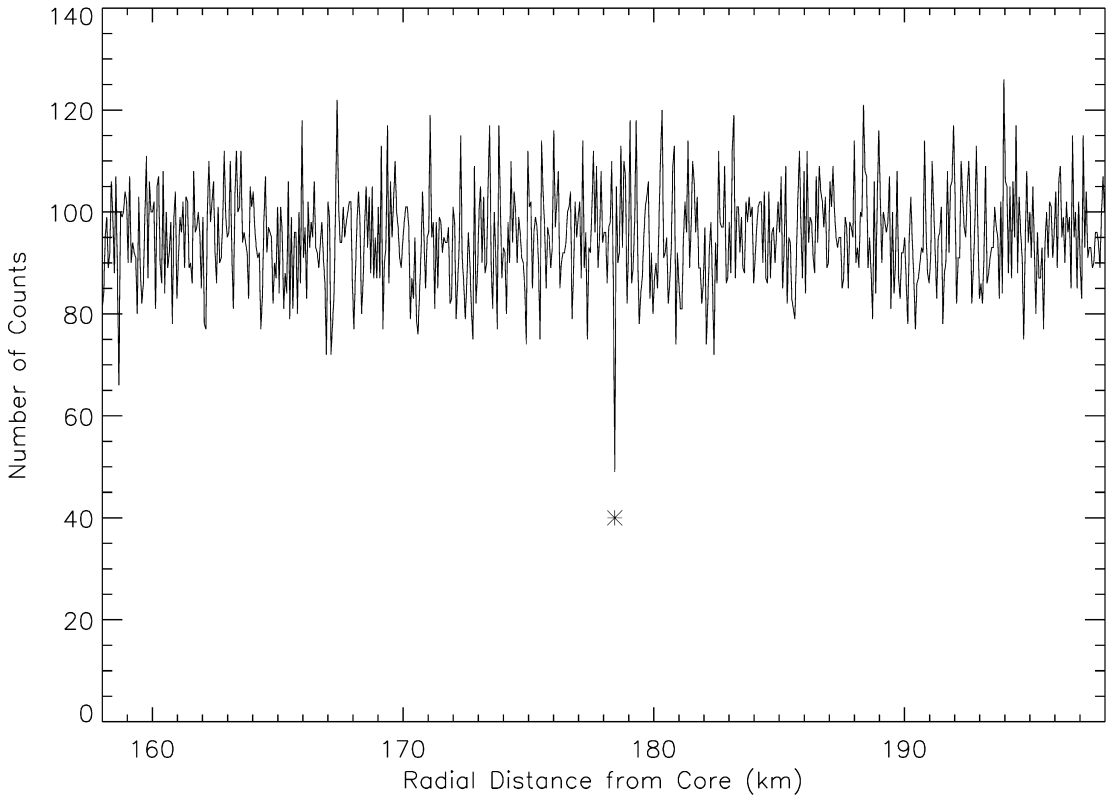

Fig. 11. Occultation data from beta Per (rev 42). Feature 12 is marked with an asterisk.

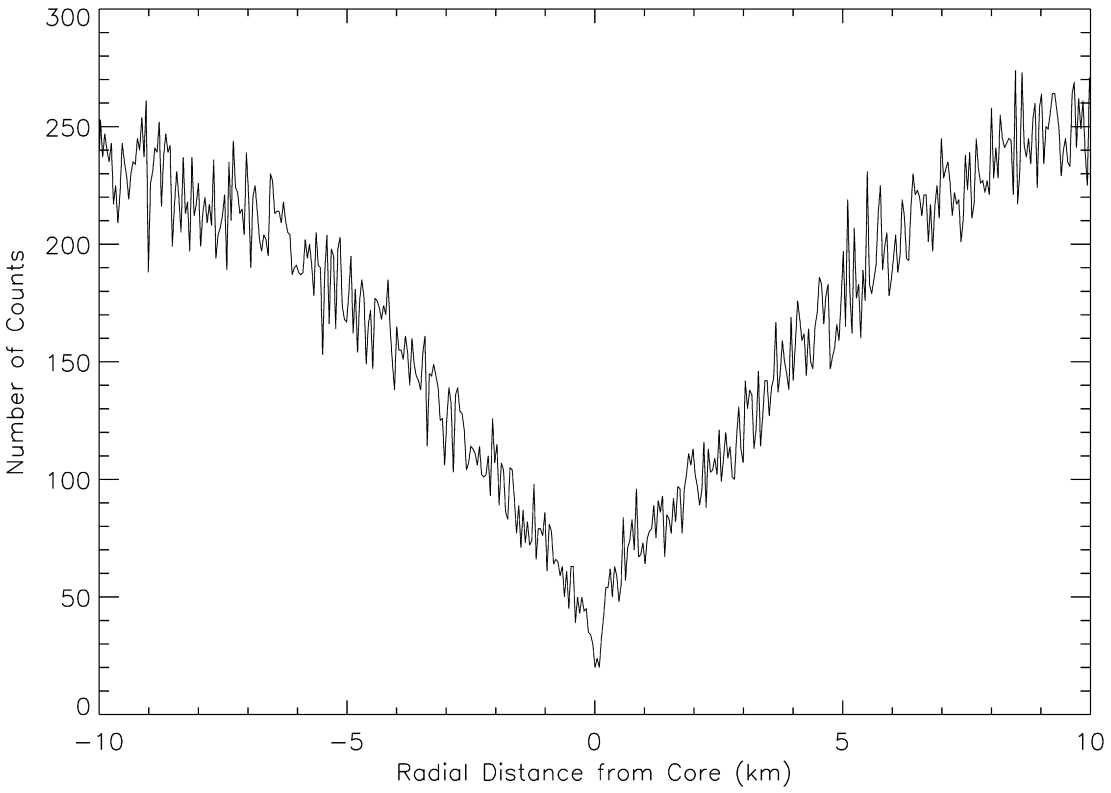

Fig. 12. Occultation data from zeta Oph (rev 26). The detected feature may be just the F ring core strand, but compare the morphology to feature 9 (Fig. 6).

thus indicate temporary aggregations. Significant recycling of ring material would allow rings to be much older than estimated.

Acknowledgments

Thanks for helpful comments from Miodrag Sremcevic, Nicole Albers, Frank Spahn, Glen Stewart, Keiji Ohtsuki, Joseph Burns and Torrence Johnson. Mark Showalter and an anonymous reviewer made numerous useful suggestions. This research was supported by the Cassini Project.

References

Altobelli, N., 2006. Presented at Cassini Rings Working Group Workshop, Kalispell, Montana, 9 August.

Barbara, J.M., Esposito, L.W., 2002. Moonlet collisions and the effects of tidally modified accretion in Saturn's F ring. Icarus 160, 161–171.

Bosh, A.S., Rivkin, A.S., 1996. Observations of Saturn's inner satellites during the May 1995 ring-plane crossing. Science 272, 518–521.

Bosh, A.S., Olkin, C.B., French, R.G., Nicholson, P.D., 2002. Saturn's F ring: Kinematics and particle sizes from stellar occultation studies. Icarus 157, 57–75.

Brown, R.H., Baines, K.H., Bellucci, G., Bibring, J.-P., Buratti, B.J., Capaccioni, F., Cerroni, P., Clark, R.N., Coradini, A., Cruikshank, D.P., Drossart, P., Formisano, V., Jaumann, R., Langevin, Y., Matson, D.L., Mccord, T.B., Mennella, V., Miller, E., Nelson, R.M., Nicholson, P.D., Sicardy, B., Sotin, C., 2004. The Cassini Visual and Infrared Mapping Spectrometer (VIMS) investigation. Space Sci. Rev. 115, 111–168.

Brown, R.H., Baines, K.H., Bellucci, G., Buratti, B.J., Capaccioni, F., Cerroni, P., Clark, R.N., Coradini, A., Cruikshank, D.P., Drossart, P., Formisano, V., Jaumann, R., Langevin, Y., Matson, D.L., McCord, T.B., Mennella, V., Nelson, R.M., Nicholson, P.D., Sicardy, B., Sotin, C., Baugh, N., Griffith, C.A., Hansen, G.B., Hibbitts, C.A., Momary, T.W., Showalter, M.R., 2006. Observations in the Saturn system during approach and orbital insertion, with Cassini's Visual and Infrared Mapping Spectrometer (VIMS). Astron. Astrophys. 446, 707–716.

Burns, J.A., Tiscareno, M.S., 2005. Saturn's ring images/dynamics by Cassini. Presented at 2005 AGU, San Francisco, 5–9 December.

Canup, R.M., Esposito, L.W., 1995. Accretion in the Roche zone: Coexistence of rings and ringmoons. Icarus 113, 331–352.

Canup, R.M., Esposito, L.W., 1997. Evolution of the G ring and the population of macroscopic ring particles. Icarus 126, 28–41.

Chambers, L.S., Cuzzi, J.N., Asphaug, E., Colwell, J.E., Sugita, S., 2007. Hydrodynamical and radiative transfer modeling of meteoroid impacts into Saturn's rings. Icarus, in press.

Colwell, J.E., Esposito, L.W., 1992. Origins of the rings of Uranus and Neptune. I. Statistics of satellite disruptions. J. Geophys. Res. Planets 97, 10227–10241.

Colwell, J.E., Horn, L.J., Lane, A.L., Esposito, L.W., Yanamandra-Fisher, P.A., Pilorz, S.H., Simmons, K.E., Morrison, M.D., Hord, C.W., Nelson, R.M., Wallis, B.D., West, R.A., Buratti, B.J., 1990. Voyager photopolarimeter observations of uranian ring occultations. Icarus 83, 102–125.

Colwell, J.W., Esposito, L.W., Bundy, D., 2000. Fragmentation rates of small satellites in the outer Solar System. J. Geophys. Res. 105, 17589–17599.

Colwell, J.E., Esposito, L.W., Sremcevic, M., 2006. Gravitational wakes in Saturn's A ring measured by stellar occultations from Cassini. Geophys. Res. Lett. 33. L07201.

Colwell, J.E., Esposito, L.W., Sremcevic, M., McClintock, W.E., Stewart, G.R., 2007. Self-gravity wakes and radial structure of Saturn's B ring. Icarus 190, 127–144.

Cuzzi, J.N., Burns, J.A., 1988. Charged particle depletion surrounding Saturn's F ring: Evidence for a moonlet belt? Icarus 74, 284–324.

Cuzzi, J.N., Estrada, P.R., 1998. Compositional evolution of Saturn's rings due to meteoroid bombardment. Icarus 132, 1–35.

Dones, L.R., 1991. A recent cometary origin for Saturn's rings? Icarus 92, 194–203.

Esposito, L.W., 1986. Structure and evolution of Saturn's rings. Icarus 67, 345–357.

Esposito, L.W., 1991. Planetary rings: Ever decreasing circles. Nature 354, 107.
Esposito, L.W., 2006. Cassini observations and ring history. Presented at European Geosciences Union, Vienna, 4 April.
Esposito, L.W., Colwell, J.E., 1989. Creation of the Uranus rings and dust bands. Nature 339, 605–607.
Esposito, L.W., Colwell, J.E., 2003. Estimating the effectiveness of cosmic recycling in the history of the planetary rings and ring moons. Presented at Fall AGU, San Francisco.
Esposito, L.W., Colwell, J.E., 2004. Explaining radial spectral variations. Presented at Fall AGU, San Francisco.
Esposito, L.W., Colwell, J.E., 2005. Cassini observations and ring history. Presented at Fall AGU, San Francisco.
Esposito, L.W., Colwell, J.E., McClintock, W.E., 1998. Cassini UVIS observations of Saturn's rings. Planet. Space Sci. 46, 1221–1235.
Esposito, L.W., Barth, C.A., Colwell, J.E., Lawrence, G.M., McClintock, W.E., Stewart, A.I.F., Keller, H.U., Korth, A., Lauche, H., Festou, M.C., Lane, A.L., Hansen, C.J., Maki, J.N., West, R.A., Jahn, H., Reulke, R., Warlich, K., Shemansky, D.E., Yung, Y.L., 2004. The Cassini Ultraviolet Imaging Spectrograph investigation. Space Sci. Rev. 115, 294–361.
Esposito, L.W., Colwell, J.E., Larsen, K., McClintock, W.E., Stewart, A.I.F., Tew Hallett, J., Shemansky, D.E., Ajello, J.M., Hansen, C.J., Hendrix, A.R., West, R.A., Keller, H.U., Korth, A., Pryor, W.R., Reulke, R., Yung, Y.L., 2005. Ultra-violet imaging spectroscopy shows an active Saturn system. Science 307, 1251–1255.
Hedman, M.M., Nicholson, P.D., Salo, H., Wallis, B.D., Burratti, B.J., Baines, K.H., Brown, R.H., Clark, R.N., 2007. Self-gravity wake structures in Saturn's A ring revealed by Cassini-VIMS. Astron. J. 133, 2624–2629.
Karjalainen, R., 2007. Aggregate impacts in Saturn's rings. Icarus 189, 523–537.
Lane, A.L., Hord, C.W., West, R.A., Esposito, L.W., Coffeen, D.L., Sato, M., Simmons, K.E., Pomphrey, R.B., Morris, R.B., 1982. Photopolarimetry from Voyager 2: Preliminary results on Saturn, Titan, and the rings. Science 215, 537–543.
Murray, C.D., 2006. Presented at Cassini Rings Working Group Workshop, Kalispell, Montana, 9 August.
Murray, C.D., Gordon, M.K., Giuliatti-Winter, S.M., 1997. Unraveling the strands of Saturn's F ring. Icarus 129, 304–316.
Nicholson, P.D., Showalter, M.R., Dones, L., French, R.G., Larson, S.M., Lissauer, J.J., McGhee, C.A., Seitzer, P., Sicardy, B., Danielson, G.E., 1996. Observations of Saturn's ring-plane crossing in August and November. Science 272, 509–516.
Ohtsuki, K., 2002. Evolution of size distribution due to accretion. Paper presented at DPS meeting, Birmingham, AL, October.
Porco, C.C., 2006. Accretionary origins for Saturn's small satellites: Sizes, shapes, and numerical simulations of growth. Presented at 2006 AGU, San Francisco, 11–15 December.
Porco, C.C., Baker, E., Barbara, J., Beurle, K., Brahic, A., Burns, J.A., Charnoz, S., Cooper, N., Dawson, D.D., Del Genio, A.D., Denk, T., Dones, L., Dyudina, U., Evans, M.W., Giese, B., Grazier, K., Helfenstein, P., Ingersoll, A.P., Jacobson, R.A., Johnson, T.V., McEwen, A., Murray, C.D., Neukum, G., Owen, W.M., Perry, J., Roatsch, T., Spitale, J., Squyres, S., Thomas, P., Tiscareno, M., Turtle, E., Vasavada, A.R., Veverka, J., Wagner, R., West, R., 2005. Cassini imaging science: Initial results on Saturn's rings and small satellites. Science 307 (5713), 1226–1236.
Porco, C.C., Thomas, P.C., Weiss, J.W, Richardson, D.C., 2007. Physical characteristics of Saturn's small satellites provide clues to their origins. Science, in press.
Poulet, F., Sicardy, B., Nicholson, P.D., Karkoschka, E., Caldwell, J., 2000. Saturn's ring-plane crossings of August and November 1995: A model for the new F-ring objects. Icarus 144, 135–148.
Showalter, M.R., 1998. Detection of centimeter-sized meteoroid impact events in Saturn's F ring. Science 282, 1099–1102.
Showalter, M.R., 2004. Disentangling Saturn's F ring. I. Clump orbits and lifetimes. Icarus 171, 356–371.
Showalter, M.R., Pollack, J.B., Ockert, M.E., Doyle, L.R., Dalton, J.B., 1992. A photometric study of Saturn's F ring. Icarus 100, 394–411.
Shu, F.H., Stewart, G.R., 1985. The collisional dynamics of particulate disks. Icarus 62, 360–383.
Smith, B.A., Soderblom, L., Batson, R.M., Bridges, P.M., Inge, J.L., Masursky, H., Shoemaker, E., Beebe, R.F., Boyce, J., Briggs, G., Bunker, A., Collins, S.A., Hansen, C., Johnson, T.V., Mitchell, J.L., Terrile, R.J., Cook, A.F., Cuzzi, J.N., Pollack, J.B., Danielson, G.E., Ingersoll, A.P., Davies, M.E., Hunt, G.E., Morrison, D., Owen, T., Sagan, C., Veverka, J., Strom, R., Suomi, V.E., 1982. A new look at the Saturn system: The Voyager 2 images. Science 215, 504–537.
Spahn, F., Sremcevic, M., 2000. Density patters induced by small moonlets embedded in Saturn's rings. Astron. Astrophys. 358, 368–372.
Spahn, F., Wiebicke, H.-J., 1989. Long-term gravitational influence of moonlets in Saturn's rings. Icarus 77, 124–134.
Srama, R., Kempf, S, Moragas-Klostermeyer, G., Beckmann, U., Postberg, F., Economou, T., Helfert, S., Spahn, F., Altobelli, N., Gruen, E., 2006. Saturn's dust environment: Experience from a two-year survey with CDA. Presented at Europlanet Conference, Berlin, 19 September.
Sremcevic, M., Spahn, F., Duschl, W.J., 2002. Density structures in perturbed thin cold discs. Mon. Not. R. Astron. Soc. 337, 1139–1152.
Sremcevic, M., Esposito, L.W., Colwell, J.E., 2006. Size of particles and clumps in saturnian rings inferred from Cassini UVIS occultations. Presented at European Geosciences Union, Vienna, 4 April.
Sremcevic, M., Schmidt, J., Salo, H., Seiss, M., Spahn, F., Albers, N., 2007. A belt of moonlets in Saturn's A ring. Nature 499, 1019–1021.
Throop, H.B., Esposito, L.W., 1998. G ring particle sizes derived from ring plane crossing observations. Icarus 131, 152–166.
Tiscareno, M.S., Burns, J.A., Hedman, M.M., Porco, C.C., Weiss, J.W., Dones, L., Richardson, D.C., Murray, C.D., 2006. 100-metre-diameter moonlets in Saturn's A ring from observations of 'propeller' structures. Nature 440, 648–650.
Tiscareno, M.S., Burns, J.A., Nicholson, P.D., Hedman, M.M., Porco, C.C., 2007. Cassini imaging of Saturn's rings II: A wavelet technique for analysis of density waves and other radial structure in the rings. Icarus 189, 14–34.
Tyler, G.L., Eshleman, V.R., Anderson, J.D., Levy, G.S., Lindal, G.F., Wood, G.E., Croft, T.A., 1981. Radio science investigations of the Saturn system with Voyager 1. Science 212, 201–206.